Cellular cholesterol efflux in heterozygotes for Tangier disease is markedly reduced and correlates with high density lipoprotein cholesterol concentration and particle size

Margaret E. Brousseau,* Gretchen P. Eberhart,† Josée Dupuis,§ Bela F. Asztalos,* Allison L. Goldkamp,* Ernst J. Schaefer,* and Mason W. Freeman[1,†]

Lipid Metabolism Laboratory,* JM-USDA Human Nutrition Research Center on Aging at Tufts University, Boston, MA and Department of Medicine, New England Medical Center, Boston, MA 02111; Lipid Metabolism Unit,† Massachusetts General Hospital, Boston, MA 02114; and Human Genetics Department,§ Genome Therapeutics Corporation, Waltham, MA 02453

Abstract **Tangier disease (TD), caused by mutations in the ATP-binding cassette 1 (ABC-1) gene, is a rare genetic disorder characterized by severe deficiency of high density lipoproteins (HDL) in the plasma, hypercatabolism of HDL, and defective apolipoprotein (apo)-mediated cellular cholesterol efflux. In the present study, we assessed plasma lipid concentrations, HDL particle size and subspecies, and cellular cholesterol efflux in 9 TD heterozygotes from a kindred in which the proband was homozygous for an A→C missense mutation at nucleotide 5338 of the ABC-1 transcript. Relative to age- and gender-matched controls from the Framingham Offspring Study (FOS), TD heterozygotes had significant reductions ($P < 0.000$) in HDL-C (−54% female; −40% male) and apoA-I (−33% female; −37% male) concentrations, as well as significantly less cholesterol (−68% female; −58% male) distributed in the largest HDL subclasses, H5 and H4. Consequently, HDL particle size (nm) was significantly smaller ($P < 0.000$) in TD heterozygotes (8.6 ± 0.6 female; 8.7 ± 0.1 male) relative to FOS controls (9.4 ± 0.4 female; 9.0 ± 0.3 male). Further studies demonstrated that apoA-I-mediated cellular cholesterol efflux in TD heterozygotes was essentially half that of controls (11 ± 2 vs. 20 ± 3% of total [^{3}H]cholesterol, $P < 0.001$), with strong correlations observed between cholesterol efflux and both HDL-C level (r = 0.600) and particle size (r = 0.680). In summary, our data demonstrate that apolipoprotein-mediated cholesterol efflux is aberrant in TD heterozygotes, as it is in homozygotes. This finding, along with the associations observed between HDL-C concentration, HDL particle size, and cholesterol efflux, supports the concept that plasma HDL-C levels are regulated, in part, by cholesterol efflux, which in turn influences HDL particle size and, ultimately, HDL apoA-I catabolism.**—Brousseau, M. E., G. P. Eberhart, J. Dupuis, B. F. Asztalos, A. L. Goldkamp, E. J. Schaefer, and M. W. Freeman. **Cellular cholesterol efflux in heterozygotes for Tangier disease is markedly reduced and correlates with high density lipoprotein cholesterol concentration and particle size.** ***J. Lipid Res.*** **2000.** 41: **1125–1135.**

Supplementary key words apolipoprotein • ATP-binding cassette 1 • cholesterol • efflux • lipoproteins • Tangier disease

First described by Fredrickson and colleagues in 1961 (1), Tangier disease (TD) is a rare genetic disorder characterized by severe deficiency of high density lipoproteins (HDL) in the plasma. A hallmark of this disease is the accumulation of cholesteryl esters (CE) in various tissues of the body, most notably in cells derived from the mononuclear phagocyte system, leading to hyperplastic orange tonsils, as well as to lymphadenopathy, hepatosplenomegaly, and peripheral neuropathy (2). TD homozygotes typically have plasma HDL cholesterol (C), apolipoprotein A-I (apoA-I), and low density lipoprotein (LDL) cholesterol levels that are approximately 5, 1, and 40% of normal, respectively (3), whereas the HDL-C and apoA-I levels of heterozygotes are 50% of normal (2). Although there is an overall increased incidence of coronary heart disease (CHD) in TD homozygotes (3), it is not as extensive as might be predicted on the basis of the strikingly low HDL-C concentrations. This could be due, in part, to the reduction of LDL-C levels observed in these patients or to specific alterations in HDL metabolism that result from the TD gene defect.

A number of kinetic studies utilizing radiolabeled HDL and apoA-I have been conducted to determine the metabolic basis for the hypoalphalipoproteinemia in TD (4–6). The collective results of these studies have established that the reduced levels of HDL-C in TD are directly attributable to the hypercatabolism of HDL constituents, rather than to the defective biosynthesis of HDL apolipopro-

Abbreviations: ABC-1, ATP-binding cassette 1; apo, apolipoprotein; BSA, bovine serum albumin; C, cholesterol; CE, cholesteryl ester; CHD, coronary heart disease; DMEM, Dulbecco's modified Eagle's medium; FCR, fractional catabolic rate; FOS, Framingham Offspring Study; HDL, high density lipoprotein; LDL, low density lipoprotein; MNPs, mononuclear phagocytes; NMR, nuclear magnetic resonance; TD, Tangier disease; TG, triglyceride.

[1] To whom correspondence should be addressed.

teins. Confirmation of the absence of a biosynthetic defect is provided by the fact that the apoA-I gene sequence is normal in TD patients (7, 8). More recent work has focused on defining the cellular defect observed in TD patients. The first evidence of an abnormality of cellular lipid metabolism in TD was provided by experiments showing that TD mononuclear phagocytes (MNPs) degraded internalized HDL completely in lysosomes, rather than resecreting internalized HDL particles, as did the monocytes taken from control subjects (9–11). In addition to this functional abnormality, distinct morphological defects in the Golgi apparatus and vesicular compartment have also been observed in the fibroblasts and MNPs of TD homozygotes (12). Several studies have further documented that apoA-I-mediated cholesterol efflux from TD fibroblasts is severely impaired, whereas passive desorption of cholesterol from TD cell plasma membranes to lipoprotein acceptors is intact (13–15). Brefeldin, an inhibitor of intracellular vesicular trafficking, has been shown to block apoA-I-mediated lipid efflux from normal fibroblasts (13, 16), without affecting the residual efflux in TD cells, suggesting that the impaired efflux in TD fibroblasts is due to a defect in a brefeldin-sensitive pathway. Moreover, the translocation of newly synthesized cholesterol to the plasma membrane, which is aberrant in TD cells (14, 15), is dependent on protein kinase C (14, 17), implicating impaired signal transduction in the pathogenesis of TD. This inability to properly translocate cellular lipids from intracellular stores to the plasma membrane provides a mechanistic explanation for the excess lipid deposition observed in TD cells.

While much progress has been made in our understanding of the metabolic basis of TD over the years, the molecular defect responsible for TD had remained elusive until recently. It is now known that mutations in the gene encoding ATP-binding cassette 1 (ABC-1) are the cause of TD (18–20). The search for the TD gene by genetic linkage analysis was particularly difficult because of the lack of unique biochemical markers that unambiguously distinguish TD heterozygotes. Although HDL-C levels are reduced in TD heterozygotes relative to age- and gender-matched controls, there are several genetic and environmental factors that influence HDL-C levels in the general population (21). In view of the severe impairment of apoA-I-mediated cellular cholesterol efflux seen in TD homozygotes, we hypothesized that fibroblasts from TD heterozygotes would have significantly less efflux than those of control subjects, providing a biochemical confirmation for the assignment of heterozygosity for TD. We further postulated that this diminished cholesterol efflux would result in decreased HDL particle size in heterozygous TD subjects.

In the present study, we demonstrate that *i*) HDL-C levels, HDL particle size, and α-migrating HDL subpopulations are significantly reduced in a cohort of TD heterozygotes relative to age- and gender-matched controls; *ii*) apoA-I-mediated cholesterol efflux in this cohort of TD heterozygotes is 50% of that observed in control subjects; and *iii*) cholesterol efflux in these TD heterozygotes correlates with HDL-C level and HDL particle size. These data represent an unequivocal demonstration that cellular cholesterol efflux to apoA-I is defective in TD heterozygotes, as it is in homozygotes, suggesting that the ABC-1 transporter is stoichiometrically coupled to the process of cellular cholesterol efflux.

MATERIALS AND METHODS

Subjects

The proband of the kindred presented in **Fig. 1**, individual 420, has been described elsewhere in detail (case 52) (3). Proband 420 developed neuropathy at age 25 years, CHD at age 46 years, and died of this disease at age 58 years. This patient was found to be homozygous for an A→C missense mutation at nucleotide 5338 of the ABC-1 transcript, resulting in the substitution of an uncharged amino acid, asparagine, with a positively charged one, histidine (22). This point mutation is located in a highly conserved region of the second transmembrane domain of the ABC-1 protein, suggesting that it has functional importance. The charge difference caused by this substitution could induce conformational alterations, ultimately preventing the necessary interaction between the ABC subunit and the transmembrane domain.

Individuals in this TD pedigree with HDL-C values below or at the 10th percentile of those for age- and gender-matched controls from the Lipid Research Clinics (23) and Framingham Offspring Study (FOS) (24) reference populations were designated as presumptive TD heterozygotes. One obligate heterozygote, individual 313, and 8 presumptive TD heterozygotes from this pedigree were studied, including 2 of the proband's brothers, 1 nephew, 1 paternal uncle, 3 paternal cousins (1 male, 2 female), and 1 maternal cousin (male), as shown in **Table 1**. Only 2 of these individuals, 310 and 429, the former of whom is now deceased, have established CHD. The patient's mother, individual 313, is 79 years old and does not have neuropathy or CHD. Plasma lipid, apoA-I, and HDL size data of TD heterozygotes were compared with those of age- and gender-matched subjects participating in cycle 4 of FOS, whereas data derived from HDL subpopulation analysis by two-dimensional gel lipoprotein electrophoresis were compared with those of 9 age- and gender-matched unaffected relatives from the kindred. For the plasma lipid and apoA-I comparisons, 1,911 females and 1,820 males from the FOS were used, whereas a random subset (113 females; 70 males) of this population was used in the HDL subclass analysis by nuclear magnetic resonance (NMR).

Genetic linkage and haplotyping analysis

Two-point linkage analysis was performed with the MLINK and ILINK components of the program LINKAGE (25), modeling low HDL-C as a codominant trait. The allele frequencies at each marker were estimated by the USERM13 program (26). Subsequently, haplotyping analysis was performed with SIMWALK2 software (27).

Plasma lipid and apoA-I determinations

Blood was collected into tubes containing 0.01% EDTA and centrifuged at 4°C to obtain plasma. Plasma total cholesterol (TC) and triglyceride (TG) concentrations in TD heterozygotes and in FOS controls were determined by enzymatic assays, as previously described (28). Plasma HDL-C concentrations were assessed subsequent to dextran sulfate–magnesium precipitation of apoB-containing lipoproteins by the method of Warnick, Benderson, and Albers (29). Non-HDL-C was calculated as the

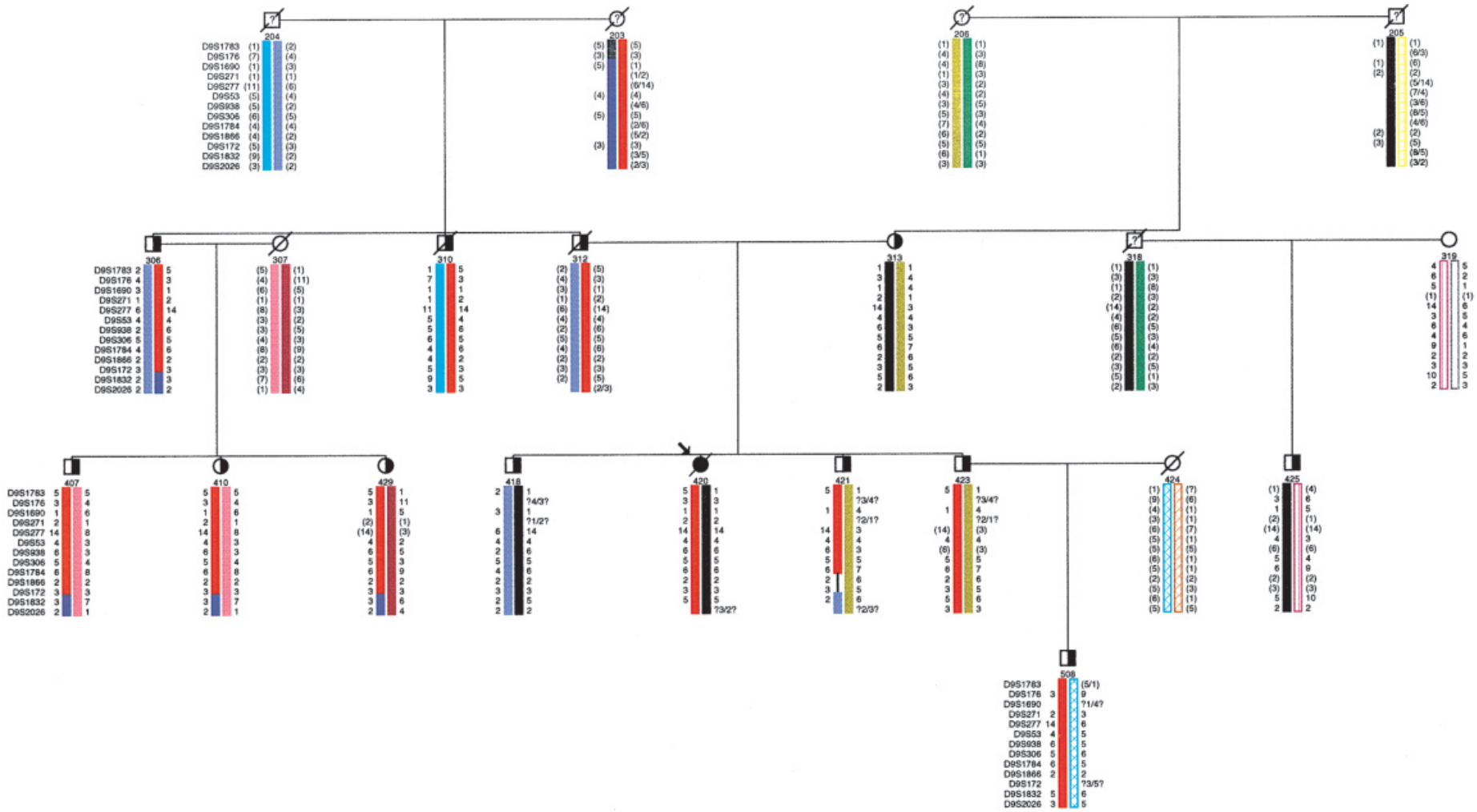

Fig. 1. Genetic analysis of TD pedigree. Squares and circles represent males and females, respectively, with heterozygosity indicated by half-shaded symbols. The location of the homozygous proband of this kindred, individual 420, is shown by a large arrow. A diagonal line through a symbol denotes that that individual is deceased. Selected microsatellite markers spanning the 9q31 region are displayed to the left of each generation. In subjects having a (?) beside a given marker, it was not possible to determine definitively from which parent alleles were derived, because they were identical in both parents. The haplotype, which can be traced through the color scheme, tracked perfectly through this subset of the pedigree, with all HDL-deficient individuals sharing the haplotype.

TABLE 1. Plasma lipid and apoA-I concentrations in Tangier disease heterozygotes and Framingham Offspring Study controls

Subject	ID Number	Age	Gender	Concentration				
				TC	HDL-C	Non-HDL-C	TG	ApoA-I
		yr				*mg/dL*		
Proband	420	56	F	137	2	135	185	2
Mother	313	79	F	194	35	159	210[a]	140
Brother	421	55	M	203	22	181	269	84
Brother	423	47	M	212	27	185	173	76
Nephew	508	13	M	124	31	93	74	95
Paternal uncle	310	89	M	145	27	118	112	100
Paternal cousin	407	50	M	134	18	116	150	71
Paternal cousin	410	35	F	209	16	193	258	77
Maternal cousin	425	55	M	225	30	195	120	85
Paternal cousin	429	53	F	246	27	219	223[a]	93
TD heterozygotes								
Mean ± SD (n = 3)		56 ± 22	F	216 ± 27	26 ± 10[b]	190 ± 30	230 ± 25[b]	103 ± 33[b]
Mean ± SD (n = 6)		52 ± 24	M	174 ± 44[c]	26 ± 5[b]	148 ± 44[c]	150 ± 68	85 ± 11[b]
FOS controls								
Mean ± SD (n = 1,911)		51 ± 10	F	206 ± 40	56 ± 15	151 ± 43	111 ± 98	154 ± 28
Mean ± SD (n = 1,820)		52 ± 10	M	205 ± 37	43 ± 12	162 ± 39	142 ± 104	134 ± 23

[a] Nonfasting triglyceride concentration.
[b] $P < 0.000$; [c] $P < 0.01$, versus age- and gender-matched controls from cycle 4 of FOS.

difference between TC and HDL-C. ApoA-I concentrations in the plasma were measured with a Spectrum CCX analyzer (Abbott Diagnostics, Abbott Park, IL) with an immunoturbidometric assay using reagents and calibrators from Incstar (Stillwater, MN) (24).

HDL subclass concentrations and particle size analysis by NMR

The distribution of HDL subclasses and HDL particle size were determined by proton NMR spectroscopy, as previously described (30, 31). The concentrations of 5 HDL subclasses are provided by this methodology: H5, H4, H3, H2, and H1, listed from largest to smallest with respect to HDL particle size. Specifically, H5 and H4 are categorized as large HDL (8.8–13.0 nm), H3 and H2 as intermediate HDL (7.8–8.8 nm), and H1 as small HDL (7.3–7.7 nm). Concentrations of HDL subclasses are expressed in units of cholesterol (mg/dL). HDL subclass distributions determined by NMR have been shown to correlate closely with those obtained by gradient gel electrophoresis (30).

HDL subpopulation analysis by two-dimensional gel lipoprotein electrophoresis

The distribution of HDL subpopulations was determined by nondenaturing two-dimensional agarose–polyacrylamide gel electrophoresis as previously described (32, 33). Electrophoretic transfer, fixing, blocking, and immunolocalization with antiserum directed against human apoA-I were also performed as described (34), and bound radioactivity was quantified by PhosphorImager analysis (Molecular Dynamics, Sunnyvale, CA). With this system, we are able to separate and quantify the following apoA-I-containing HDL subpopulations: pre-β, α, and pre-α. Criteria for designation of α1, α2, and α3 HDL subfractions are based on integration of α-migrating HDL in the two-dimensional system. Three distinct peaks are observed, providing a basis for the designation of the subfractions (34). Concentrations of apolipoproteins within the HDL subpopulations were calculated by multiplying the percent distribution of the apoA-I-containing HDL subpopulation with the plasma concentration of apoA-I. ^{125}I-labeled high molecular weight standard proteins (Pharmacia, Piscataway, NJ) were applied simultaneously with the plasma samples to each 3–34% gradient polyacrylamide gel in the second dimension to determine the size of HDL subpopulations.

Lipoprotein and apolipoprotein isolation

HDL_2 and HDL_3 were prepared by sequential ultracentrifugation of normal plasma in the density intervals of 1.063 to 1.125 and 1.125 to 1.21 g/mL, respectively, using standard methods (35). HDL_3 was passed over a heparin–agarose type 1 column (Sigma Chemicals, St. Louis, MO) to remove apoE. ApoA-I was isolated from delipidated HDL_2 as described (36). Protein was measured by the method of Lowry et al. (37).

Cell culture

Fibroblast lines were initiated by explant culture from a 3-mm punch biopsy at a 1-mm skin thickness obtained under sterile conditions from the medial aspect of the inner arm and placed in HEPES-buffered saline, pH 7.4. The tissue was transferred to a 100-mm sterile plastic petri dish and diced. Explants were transferred to 25-cm^2 flasks in Dulbecco's modified Eagle's medium (DMEM) with 15% fetal bovine serum (FBS), penicillin (50 U/mL), and streptomycin (50 μg/mL). Explant culture was performed either in the Cytogenetics Laboratory of the Brigham and Women's Hospital (Boston, MA) or in the Cytogenetics Department of the New England Medical Center (NEMC, Boston, MA). Two control primary fibroblast cell lines from the former laboratory, 1 from the NEMC laboratory, and 2 from the American Type Culture Collection (Rockville, MD) were used for the comparison studies. All fibroblasts were used between passage 5 and 12.

Cholesterol loading and labeling of cells

Fibroblasts were grown to 60–80% confluence in DMEM with 10% FBS and labeled by incubating in medium with 0.2–0.5 μCi of [^{3}H]cholesterol per mL (New England Nuclear, Boston, MA) until confluent, approximately 72 h. Labeled cells were cholesterol enriched by incubation in DMEM with fatty acid-free bovine serum albumin (DMEM/FAF-BSA, 2 mg/mL) and nonlipoprotein cholesterol (30 μg/mL) from an ethanol stock solution for 24 h. Cells were incubated for 48 h in DMEM with FAF-BSA (1 mg/mL) to allow cellular cholesterol pools to equilibrate (38), before the initiation of the efflux measurements.

Measuring cellular cholesterol efflux

Efflux of radiolabeled cholesterol from cells was measured as previously described (39). Briefly, cholesterol-loaded [^{3}H]cho-

lesterol-labeled cells were incubated in DMEM/FAF-BSA with increasing levels of apoA-I for 16 h at 37°C. After incubation with acceptors, efflux medium was removed and centrifuged to remove cells and debris, and an aliquot of medium was counted directly in a scintillation counter. After washing with phosphate-buffered saline (PBS), cell lipids were extracted from culture dishes with hexane–isopropanol 3:2 (v/v), and then evaporated to dryness under nitrogen gas, reconstituted in chloroform, and subjected to thin-layer chromatography. Cell proteins were dissolved in 0.1 N NaOH and aliquots quantified by the method of Lowry. The amount of cholesterol appearing in the medium was expressed as a percentage of the sum of [^{3}H]cholesterol found in the medium and in cellular unesterified and esterified cholesterol.

Statistical analysis

The SYSTAT statistical program (SPSS 9.0 for Windows; SPSS, Chicago, IL) was used for all analyses. Mean differences between TD heterozygotes and control subjects were assessed for statistical significance ($P < 0.05$) with unpaired *t*-tests. Correlation coefficients were determined by the method of Pearson.

RESULTS

Haplotyping analysis

The results of haplotyping analysis of 13 polymorphic microsatellite markers on chromosomal band 9q31 are presented in Fig. 1. The markers are listed in Fig. 1 with respect to centromeric→telomeric boundaries. The proband, individual 420, was homozygous for all the markers presented in Fig. 1, with the exception of the first and last. The proband's mother, individual 313, was homozygous for markers D9S53 and D9S306, as were her two brothers, individuals 421 and 423. Individual 508, the proband's nephew, was heterozygous for all markers but D9S1866, whereas the proband's maternal cousin, subject 425, was homozygous for the greatest number of microsatellite markers at 4. In this pedigree, we detected a maximum LOD score of 5.15 at a recombination fraction of 0.0 at D9S1784, indicating that this particular marker was most informative in this kindred. All HDL-deficient individuals designated as presumptive heterozygotes were found to have the same haplotype.

Plasma lipid and apoA-I concentrations

The plasma lipid and apoA-I concentrations of our TD proband, 9 related TD heterozygotes (3 females, 6 males), and age- and gender-matched FOS control subjects are provided in Table 1. The proband, individual 420, had an HDL-C of 2 mg/dL, a non-HDL-C of 135 mg/dL, and fasting triglycerides of 185 mg/dL. The HDL-C level of the obligate heterozygote, the proband's mother, was 35 mg/dL, with non-HDL-C and triglyceride concentrations of 159 and 210 mg/dL, respectively. The proband's 2 brothers, individuals 421 and 423, also had markedly reduced concentrations of HDL-C and apoA-I. The remaining 6 relatives had HDL-C levels ranging from 16 mg/dL in a 35-year-old female cousin to 31 mg/dL in a 13-year-old nephew. Comparable reductions were observed in plasma apoA-I concentrations.

As compared with age- and gender-matched controls from the Framingham Offspring Study, the 3 female TD heterozygotes from this pedigree had significantly reduced HDL-C (−54%, $P < 0.000$) and apoA-I (−33%, $P < 0.000$) concentrations, as well as a 2-fold increase in plasma triglycerides. However, because the samples from individuals 313 and 429 were obtained in the nonfasting state, the latter increase must be interpreted with caution. The 6 male TD heterozygotes also had markedly reduced HDL-C (−40%, $P < 0.000$) and apoA-I (−37%, $P < 0.000$) concentrations relative to age- and gender-matched FOS controls. In addition, both total and non-HDL cholesterol levels were significantly decreased ($P < 0.01$) in male TD heterozygotes (−15 and −9%, respectively). Plasma triglyceride concentrations were not different between male TD heterozygotes and FOS controls.

HDL subclass concentrations and particle size

Table 2 shows the results of plasma HDL subclass analysis, as assessed by NMR, in TD heterozygotes and FOS controls. The cholesterol concentrations (mg/dL) of 5 subclasses of HDL are provided for affected and unaffected individuals, with H5 having the largest particle size and H1 the smallest. The only HDL subclass that had measurable cholesterol in the proband was H1, the subclass corresponding to the smallest HDL particles. Thus, the HDL particle size of proband 420 was only 7.5 nm. The proband's mother, individual 313, had the majority (80%) of HDL-associated cholesterol distributed in the H4 and H3 subclasses, with a mean HDL particle size of 9.2 nm. Relative to age- and gender-matched FOS subjects, the female TD heterozygotes from this pedigree had significantly less cholesterol distributed in the H5 subclass (8% TD vs. 25% FOS) but approximately 2.5-fold more cholesterol distributed in the H3 (42% TD vs. 18% FOS) and H1 (23% TD vs. 9% FOS) subclasses, when expressed as a percentage of total HDL-C concentration. Overall, this resulted in a mean HDL particle diameter for female TD heterozygotes of 8.6 ± 0.6 nm which was significantly smaller than that of 9.4 ± 0.4 nm for female FOS controls. Similarly, a significant reduction in the cholesterol content of the H5 subclass was noted in male TD heterozygotes, as compared with male FOS control subjects (8% TD vs. 19% FOS). A 2-fold increase in the level of H1 cholesterol was also observed in male TD heterozygotes relative to controls (19% TD vs. 9% FOS). The preceding differences in HDL cholesterol subclass distribution resulted in a mean HDL particle size for male TD heterozygotes of 8.7 ± 0.1 nm, which was significantly smaller than that of 9.0 ± 0.3 nm for FOS males.

HDL subpopulation analysis by two-dimensional gel lipoprotein electrophoresis

To characterize further the HDL subpopulations of TD heterozygotes, we performed nondenaturing two-dimensional gel electrophoresis. Data for the 9 TD heterozygotes, as well as 9 age- and gender-matched relatives, are presented in **Table 3**. In this methodology, HDL subpopulations are defined by size and charge, with pre-β-migrating HDL being smaller and lipid poor relative to α-

TABLE 2. Plasma HDL subclass concentrations and particle size in Tangier disease heterozygotes and Framingham Offspring Study controls

ID Number	Concentration						HDL Size
	HDL-C	H5[a]	H4	H3	H2	H1	
	mg/dL						*nm*
420	2	0	0	0	0	1	7.5
313	35	4	13	15	0	3	9.2
421	22	2	0	18	0	4	8.6
423	27	4	10	8	5	9	8.8
508	31	3	7	8	3	11	8.7
310	27	2	0	10	10	2	8.6
407	18	2	0	13	2	1	8.8
410	16	0	4	0	0	8	8.1
425	27	0	19	5	0	4	8.9
429	30	1	3	19	0	6	8.5
TD heterozygotes							
Female mean ± SD	26 ± 10[b]	2 ± 2[b]	7 ± 6[c]	11 ± 10	0 ± 0[b]	6 ± 3	8.6 ± 0.6[b]
(n = 3)		(8%)	(27%)	(42%)	(0%)	(23%)	
		[−86%]	[−57%]	[+10%]	[100%]	[+20%]	
Male mean ± SD	26 ± 5[b]	2 ± 1[c]	6 ± 7[d]	10 ± 5	3 ± 4[b]	5 ± 4[c]	8.7 ± 0.1[c]
(n = 6)		(8%)	(23%)	(39%)	(12%)	(19%)	
		[−75%]	[−33%]	[−17%]	[−70%]	[−44%]	
FOS Controls							
Female mean ± SD	56 ± 15	14 ± 8	17 ± 10	10 ± 6	11 ± 6	5 ± 4	9.4 ± 0.4
(n = 113)		(25%)	(30%)	(18%)	(20%)	(9%)	
Male mean ± SD	43 ± 12	8 ± 4	9 ± 8	12 ± 5	10 ± 7	9 ± 5	9.0 ± 0.3
(n = 70)		(19%)	(21%)	(28%)	(23%)	(9%)	

[a] H5 has the largest particle size followed by H4 > H3 > H2 > H1. Values in parentheses represent the percent contribution of the subclass relative to the total HDL-C concentration, while values in brackets represent the percent difference from FOS controls.
[b] $P < 0.000$, versus age- and gender-matched controls from cycle 4 of FOS.
[c] $P < 0.001$, versus age- and gender-matched controls from cycle 4 of FOS.
[d] $P < 0.03$, versus age- and gender-matched controls from cycle 4 of FOS.

and pre-α-migrating HDL. No significant differences were observed in the apoA-I-containing pre-β-migrating HDL subpopulations of TD heterozygotes as compared with age- and gender-matched relatives. The most dramatic differences noted between the affected and unaffected family members occurred in the α-migrating HDL subpopulations. The mean concentration of the largest α-migrating HDL subpopulation, α1, was substantially reduced (−71%) in TD heterozygotes relative to unaffected subjects. This was similarly the case for the α2 HDL subpopulation, the mean level (mg/dL) of which was 34 ± 10 in TD heterozygotes versus 49 ± 16 in unaffected relatives. Concentrations of the α3 HDL subpopulation were also reduced in TD heterozygotes, with the 23% reduction just failing to achieve statistical significance ($P = 0.06$). Reductions were also observed in the concentrations of pre-α-migrating HDL subpopulations when the 2 groups were compared. The mean concentration of pre-α1-migrating HDL was 67% lower in TD heterozygotes than in unaffected family members, while those of pre-α2 and pre-α3 were each reduced by 50%. Interestingly, the percent distribution of apoA-I-containing HDL subpopulations was not dramatically different between affected and unaffected relatives, with the principal exception being the greater than 50% reduction in the contribution of the α1 HDL subpopulation to the total plasma apoA-I concentration in TD heterozygotes.

TABLE 3. Plasma concentrations of apoA-I-containing HDL subpopulations in Tangier disease heterozygotes and unaffected relatives

Group	Concentration							
	Pre-β1	Pre-β2	α1	α2	α3	Pre-α1	Pre-α2	Pre-α3
	mg/dL							
TD heterozygotes	9 ± 8	3 ± 2	7 ± 4[a]	34 ± 10[b]	33 ± 6	1 ± 1[c]	2 ± 1[b]	1 ± 1
(n = 9)	(10%)	(3%)	(8%)	(37%)	(37%)	(1%)	(3%)	(2%)
	[−39%]	[−25%]	[−71%]	[−31%]	[−23%]	[−67%]	[−50%]	[−50%]
Unaffected relatives	13 ± 9	4 ± 2	24 ± 9	49 ± 16	43 ± 13	3 ± 1	4 ± 1	2 ± 1
(n = 9)	(9%)	(3%)	(17%)	(34%)	(30%)	(2%)	(3%)	(1%)

Values in parentheses represent the percent contribution of each apoA-I-containing HDL subpopulation to the total plasma apoA-I concentration, while values in brackets represent the percent difference from the mean value of unaffected relatives.
[a] $P < 0.001$; [b] $P < 0.005$; [c] $P < 0.01$.

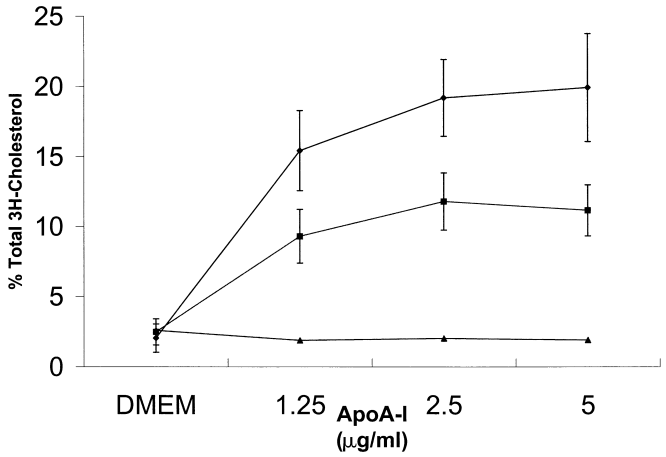

Fig. 2. Cholesterol efflux from the fibroblasts of TD homozygote 420 (solid triangles), related TD heterozygotes (solid squares, n = 9), and control subjects (solid diamonds, n = 5). Subconfluent cells were labeled with [^{3}H]cholesterol, followed by incubation with exogenous unlabeled cholesterol. Efflux was performed in triplicate for each individual, with apoA-I concentrations in the medium ranging from 0 to 5 μg/mL. Efflux medium was then counted, cell lipids extracted, and extracts separated by TLC for the isolation of esterified and unesterified cholesterol. Means ± SD for each apoA-I concentration are expressed as a percentage of total (medium plus cell) [^{3}H]cholesterol. * $P < 0.001$ versus mean value of control subjects.

Cellular cholesterol efflux

The ability of apoA-I to promote efflux of cholesterol from the fibroblasts of proband 420, TD heterozygotes, and control subjects is summarized in **Fig. 2**. In these studies, fibroblasts were enriched with cholesterol by incubation with nonlipoprotein cholesterol, before incubation with either albumin alone or increasing concentrations of apoA-I. Maximal cellular cholesterol efflux from the fibroblasts of our proband in the presence of apoA-I was virtually identical to that seen with albumin alone, with approximately 2% of total [^{3}H]cholesterol appearing in the medium. Maximal cellular cholesterol efflux from the cells of presumptive TD heterozygotes averaged 11 ± 2% of total [^{3}H]cholesterol. Although this was substantially greater than that from our proband, this value was significantly lower ($P < 0.001$) than that of 20 ± 3 seen in control subjects.

In **Fig. 3**, apoA-I-mediated cholesterol efflux for each of the 9 TD heterozygotes (1 obligate, 8 presumptive) is expressed relative to control subjects, with the latter assigned a value of 100%. ApoA-I-mediated cholesterol efflux was calculated as the maximal cholesterol efflux in the presence of apoA-I minus the cholesterol efflux to albumin alone**.** The percent of the control efflux value for the TD heterozygotes in this pedigree ranged from a low of 38% for individual 410 to a high of 63% for individual 429. Individual 410 also had the lowest HDL-C concentration (16 mg/dL), while individual 429 had one of the highest HDL-C levels (27 mg/dL). The mean value of percent control efflux for all 9 TD heterozygotes relative to the control value was 51 ± 10%, indicating that apolipoprotein-mediated cellular cholesterol efflux is essentially half-normal in TD heterozygotes.

Associations between HDL-C concentration, HDL particle size, and cholesterol efflux

As depicted in **Fig. 4**, correlation coefficient analysis of data from the 9 TD heterozygotes studied demonstrated that HDL-C concentration was highly correlated with HDL size (r = 0.816, $P < 0.01$). The two HDL subclasses having the largest particle size, H5 and H4, were also significantly associated with HDL-C concentration (r = 0.717, $P < 0.03$; r = 0.768, $P < 0.02$, respectively). Figure 4 also shows that cellular cholesterol efflux correlated with HDL-C level (r = 0.600, $P = 0.08$) and HDL particle size (r = 0.680, $P = 0.06$) in these individuals; however, these associations did not quite reach statistical significance because of the relatively small number of individuals studied. None of the HDL subclasses was significantly correlated with cholesterol efflux, indicating that mean HDL particle size was a better correlate of efflux than was any specific HDL subclass. This finding was likely due to the fact that the distribution of cholesterol among the HDL subclasses was similar in these individuals.

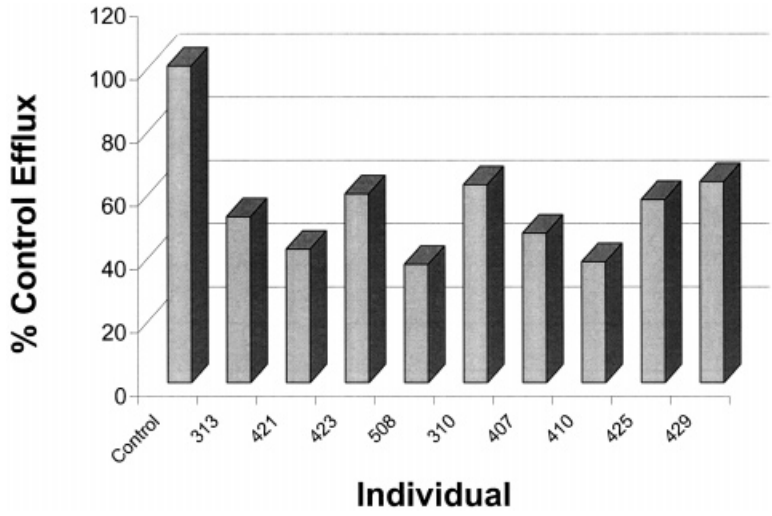

Fig. 3. ApoA-I-mediated cellular cholesterol efflux for each of the TD heterozygotes (n = 9) expressed as a percentage of the value for control subjects (n = 5), with the latter assigned a value of 100%. ApoA-I-mediated cholesterol efflux was calculated as the difference between maximal cellular cholesterol efflux in the presence of apoA-I and cholesterol efflux in the presence of albumin alone. The percentage of control efflux for the TD heterozygotes in this pedigree ranged from a low of 38% for individual 410 to a high of 63% for individual 429. The mean value for the 9 TD heterozygotes was 51 ± 10% of that for the control subjects, indicating that apoA-I-mediated cholesterol efflux is half-normal in this cohort of TD heterozygotes.

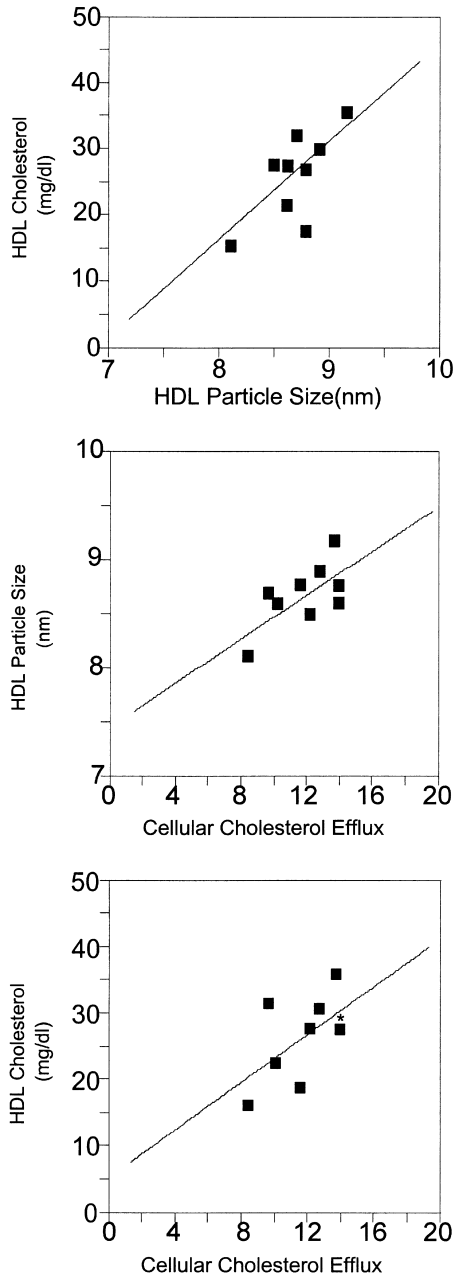

Fig. 4. Correlations between HDL-C concentration, HDL particle size, and apolipoprotein-mediated cellular cholesterol efflux in TD heterozygotes (n = 9). As shown in the upper panel, HDL-C was highly correlated with HDL particle size (r = 0.816, $P < 0.01$), as well as with cellular cholesterol efflux in the presence of apoA-I at 2.5 μg/mL (r = 0.600, $P = 0.08$; lower panel). In the lower panel, 2 subjects having overlapping values are depicted with an asterisk (*). The association between HDL particle size and cellular cholesterol efflux is displayed in the middle panel (r = 0.680, $P = 0.06$). These data suggest that cholesterol efflux to apoA-I influences HDL particle size, which, in turn, mediates HDL-C concentrations.

DISCUSSION

The data presented here represent an unequivocal demonstration of impaired apoA-I-mediated cellular cholesterol efflux in a cohort of TD heterozygotes. Within this group, apoA-I-mediated cellular cholesterol efflux ranged from 38 to 62% of that seen in control subjects and was, on average, half-normal. This report joins a growing body of evidence establishing that defective apolipoprotein-mediated cholesterol efflux is a hallmark of Tangier disease (13–15, 40). The apparent universality of abnormal cholesterol efflux seen in the TD homozygotes and heterozygotes studied to date strongly suggests that the activity of the TD gene product, ABC-1, tightly controls cellular cholesterol efflux to apoA-I.

In the present study, we observed that plasma HDL-C and apoA-I levels were appreciably lower in TD heterozygotes relative to age- and gender-matched control subjects, confirming the previous report of Assmann et al. (41). The mean HDL-C concentration for female TD heterozygotes was comparatively more diminished relative to the control group than was the reduction noted in male TD heterozygotes, −54 versus −40%, respectively, with the reduction observed in apoA-I concentrations in affected males (−37%) being slightly greater than that of affected females (−33%). In addition, only male TD heterozygotes exhibited decreases in total and nonHDL cholesterol levels as compared with FOS control subjects, suggesting that an interaction may exist between gender and ABC-1 status.

Given the diminished apoA-I-mediated cellular cholesterol efflux noted in TD heterozygotes, it might be hypothesized that these subjects would, consequently, have smaller HDL particles relative to control subjects. Data from NMR analysis presented here confirmed this hypothesis. The decrease observed in TD heterozygotes was less severe than that observed in the homozygous proband, suggesting a dose–response effect of ABC-1 and, ultimately, cholesterol efflux on HDL particle size. Further characterization of HDL subfractions by nondenaturing two-dimensional gel lipoprotein electrophoresis revealed that the greatest difference observed between affected and unaffected relatives from this kindred occurred in the α-migrating HDL subclass having the largest size, the α1 subfraction, with a 71% reduction in the former group. This finding is consistent with our HDL subclass data, determined by NMR, which similarly demonstrated that the greatest differences between TD heterozygotes and unaffected relatives of both genders were observed in the concentrations of HDL subclasses having the largest particle sizes, H5 and H4. A selective reduction in the α1 subpopulation was also the most significant difference reported in a group of men with HDL deficiency (≤35 mg/dL), as compared with those having normal HDL-C levels (42). The α1 subfraction consists solely of LpA-I particles (42), decreased levels of which have been purported to increase CHD risk (43). Thus, a reduced concentration of α1-migrating apoA-I particles may contribute to the increased risk for premature CHD associated with TD (3).

The precise mechanisms underlying the reduction in plasma HDL-C concentrations observed in TD are not fully understood. It has been postulated that reduced cellular cholesterol efflux in TD leads to smaller HDL particles that, in turn, are more rapidly cleared from the plasma compartment (40, 44). Hypercatabolism of HDL apoA-I is precisely the metabolic defect that has been re-

ported in TD homozygotes (4). This phenomenon has also been observed in TD heterozygotes, with a 2-fold increase noted in HDL apoA-I fractional catabolic rate (FCR), accounting for a 50% reduction in pool size (4). Additional support for this hypothesis includes the clear inverse relationship that exists between HDL particle size and FCR (45–49), with variations in HDL FCR shown to be a prime determinant of plasma HDL-C concentrations (46, 47, 50). Hence, our data are consistent with the concept that the impairment of apoA-I-mediated cellular cholesterol efflux seen in TD heterozygotes contributes, in part, to the reductions in HDL-C concentrations by decreasing HDL cholesterol content and, thus, HDL particle size, ultimately leading to enhanced catabolism of HDL apoA-I.

The role that ABC-1 plays in facilitating apoA-I-mediated cellular lipid efflux is unknown. Possible roles for ABC-1 include a direct interaction with apoA-I at the plasma membrane, participation in a signal transduction pathway downstream from apoA-I binding, or interactions with lipids or lipid carriers involved in the transport of cholesterol and phospholipid from intracellular stores to the plasma membrane. The latter function is suggested by the recent finding that the highly homologous transporter, Rim, appears to function as a lipid "flippase," translocating *N*-retinylidene phosphatidylethanolamine in photoreceptor rod outer segment disks to the outer leaflet of the plasma membrane (51). Moreover, phospholipid efflux has clearly been shown to be defective in TD homozygotes (13, 52, 53), further implicating ABC-1 not only in cellular cholesterol metabolism but in phospholipid metabolism as well. If the lipid transport process involving ABC-1 requires a stoichiometric coupling of the transporter to the transported lipid, it could account for the half-normal cholesterol efflux seen in the TD heterozygotes we studied.

The results of correlation coefficient analysis in our study confirmed a strong association between HDL-C concentration and HDL particle size amongst this group of TD heterozygotes, with an r value of 0.816. This indicates that HDL particle size was an important determinant of HDL-C concentration in this group. TD heterozygotes with the highest HDL-C levels tended to be those with the greatest cellular cholesterol efflux values. In addition, cellular cholesterol efflux in TD heterozygotes positively correlated with both HDL-C concentration and HDL particle size, providing further evidence that cellular cholesterol efflux mediates HDL particle size, and, in turn, plasma HDL-C concentration. It is clear from these data that ABC-1 status has a significant impact on both cholesterol efflux and HDL-C concentration in this population. Whether variations in ABC-1 expression or activity could underlie some of the population variability in HDL-C levels is an intriguing question. One study has reported that two loci, one on chromosome 8 and the other on chromosome 15, affect HDL-C levels in large, randomly assigned pedigrees (54). Neither of these loci is affiliated with any presently established determinants of HDL-C concentrations, such as lipid enzymes or receptors. Thus, defining the influence of polymorphisms in the ABC-1 gene on HDL-C concentrations in the general population, as well as in those with common HDL deficiencies, could contribute substantially to our knowledge of sources for variation in HDL-C concentrations.

In summary, our data demonstrate that apolipoprotein-mediated cellular cholesterol efflux is defective in a cohort of TD heterozygotes, as it is in homozygotes. Moreover, HDL-C concentration, HDL particle size, and α-migrating HDL subspecies were significantly reduced in TD heterozygotes relative to age- and gender-matched control subjects, with the former two variables correlating with the degree of cholesterol efflux. These defects were less severe than those observed in the homozygous TD proband, suggesting a dosage effect of the TD gene product, ABC-1, on these parameters. The preceding findings, along with the associations observed between cellular cholesterol efflux, HDL particle size, and HDL-C concentration, support the concept that plasma HDL-C levels are regulated, in part, by cellular cholesterol efflux that, in turn, influences HDL particle size and, ultimately, HDL apoA-I catabolism. Larger population studies will be required to ascertain the relevance of the relationships between ABC-1 genotype, HDL particle size, and variations in plasma HDL-C concentrations in the general population.

The authors thank Nancy Neyhard for excellent technical assistance, as well as Dr. José M. Ordovas, Dr. James Otvos, and Dr. Paul Van Eerdewegh for their valuable contributions to this work. This research was supported by the Patricia Isaia Research Fund (E.J.S.), a contract from the Genome Therapeutics Corporation (E.J.S.), and NIH awards HL-09319 and HL-45098 (M.W.F.).

Manuscript received 14 October 1999 and in revised form 6 April 2000.

REFERENCES

1. Fredrickson, D. S., P. H. Altrocchi, L. V. Avioli, D. S. Goodman, and H. C. Goodman. 1961. Tangier disease. *Ann. Intern. Med.* **55:** 1016–1031.
2. Assmann, G., A. von Eckardstein, and H. B. Brewer, Jr. 1995. *In* The Metabolic and Molecular Basis of Inherited Disease. C. R. Scriver, A. L. Beaudet, W. S. Sly, and D. Valle, editors. McGraw-Hill, New York. 2053–2072.
3. Serfaty-Lacrosniere, C., F. Civeira, A. Lanzberg, P. Isaia, J. Berg, E. D. Janus, M. P. Smith, Jr., P. H. Pritchard, J. Frohlich, R. S. Lees, G. F. Barnard, J. M. Ordovas, and E. J. Schaefer. 1994. Homozygous Tangier disease and cardiovascular disease. *Atherosclerosis.* **107:** 85–98.
4. Schaefer, E. J., C. B. Blum, R. I. Levy, L. L. Jenkins, P. Alaupovic, D. M. Foster, and H. B. Brewer, Jr. 1978. Metabolism of high-density lipoprotein apolipoproteins in Tangier disease. *N. Engl. J. Med.* **299:** 905–910.
5. Schaefer, E. J., D. W. Anderson, L. A. Zech, F. T. Lindren, T. J. Bronzert, E. A. Rubalcaba, and H. B. Brewer, Jr. 1981. Metabolism of high density lipoprotein subfractions and constituents in Tangier disease following the infusion of high density lipoproteins. *J. Lipid Res.* **22:** 217–228.
6. Bojanovski, D., R. E. Gregg, L. A. Zech, M. S. Meng, C. Bishop, R. Ronan, and H. B. Brewer, Jr. 1987. In vivo metabolism of proapolipoprotein A-I in Tangier disease. *J. Clin. Invest.* **80:** 1742–1747.
7. Law, S. W., and H. B. Brewer, Jr. 1985. Tangier disease: the complete mRNA sequence encoding for preproapo-A-I. *J. Biol. Chem.* **260:** 12810–12814.
8. Makrides, S. C., N. Ruiz-Opazo, A. L. Hayden Nussbaum, J. L. Breslow, and V. I. Zannis. 1988. Sequence and expression of Tangier apoA-I gene. *Eur. Biochem.* **173:** 465–471.

9. Schmitz, G., G. Assmann, H. Robenek, and B. Brennhausen. 1985. Tangier disease: a disorder of intracellular membrane traffic. *Proc. Natl. Acad. Sci. USA.* **82:** 6305–6309.
10. Schmitz, G., H. Robenek, U. Lohmann, and G. Assmann. 1985. Interaction of high density lipoproteins with cholesteryl ester laden macrophages: biochemical and morphological characterization of cell surface binding, endocytosis and resecretion of high density lipoproteins by macrophages. *EMBO J.* **4:** 613–622.
11. Alam, R., F. M. Yatsu, L. Tsu, and S. Alam. 1989. Receptor-mediated uptake and "retroendocytosis" of high-density lipoproteins by cholesterol-loaded human monocyte-derived macrophages: possible role in enhancing reverse cholesterol transport. *Biochim. Biophys. Acta.* **1004:** 292–299.
12. Robenek, H., and G. Schmitz. 1991. Abnormal processing of Golgi elements and lysosomes in Tangier disease. *Arterioscler. Thromb.* **11:** 1007–1020.
13. Remaley, A. T., U. K. Schumacher, J. A. Stonik, B. D. Farsi, H. Nazih, and H. B. Brewer, Jr. 1997. Decreased reverse cholesterol transport from Tangier disease fibroblasts: acceptor specificity and effect of brefeldin on lipid efflux. *Arterioscler. Thromb. Vasc. Biol.* **17:** 1813–1821.
14. Walter, M., U. Gerdes, U. Seedorf, and G. Assmann. 1994. The high density lipoprotein and apolipoprotein A-I induced mobilization of cellular cholesterol is impaired in fibroblasts from Tangier disease subjects. *Biochem. Biophys. Res. Commun.* **205:** 850–856.
15. Rogler, G., B. Trumbach, B. Klima, K. J. Lackner, and G. Schmitz. 1995. HDL-mediated efflux of intracellular cholesterol is impaired in fibroblasts from Tangier disease patients. *Arterioscler. Thromb. Vasc. Biol.* **15:** 683–690.
16. Mendez, A. J. 1995. Monensin brefeldin A inhibit high density lipoprotein-mediated cholesterol efflux from cholesterol-enriched cells. *J. Biol. Chem.* **270:** 5891–5900.
17. Forte, T. M., R. Goth-Goldstein, R. W. Nordhausen, and M. R. McCall. 1993. Apolipoprotein A-I cell membrane interaction: extracellular assembly of heterogeneous nascent HDL particles. *J. Lipid Res.* **34:** 317–324.
18. Bodzioch M., E. Orso, J. Klucken, T. Langmann, X. Böttcher, W. Diedereich, W. Drobnik, S. Barlage, C. Büchler, M. Porsch-Özcürümez, W. E. Kaminski, H. W. Hahmann, K. Oette, G. Rothe, C. Aslanidis, K. H. Lackner, and G. Schmitz. 1999. The gene encoding ATP-binding cassette transporter 1 is mutated in Tangier disease. *Nature Genet.* **22:** 347–351.
19. Brooks-Wilson, A., M. Marcil, S. M. Clee, L-H. Zhang, K. Roomp, M. van Dam, L. Yu, C. Brewer, J. A. Collins, H. O. Molhuizen, O. Loubser, B. F. F. Ouelette, K. Fichter, K. J. D. Ashbourne-Excoffon, C. W. Sensen, S. Scherer, S. Mott, M. Denis, D. Martindale, J. Frolich, K. Morgan, B. Koop, S. Pimstone, J. J. P. Kastelein, J. Genest, Jr., and M. R. Hayden. 1999. Mutations in ABC1 in Tangier disease and familial high-density lipoprotein deficiency. *Nature Genet.* **22:** 336–345.
20. Rust, S., M. Rosier, H. Funke, J. Real, Z. Amoura, J-C. Piette, J-F. Deleuze, H. B. Brewer, Jr., N. Duverger, P. Denèfle, and G. Assmann. 1999. Tangier disease is caused by mutations in the gene encoding ATP-binding cassette transporter 1. *Nature Genet.* **22:** 352–355.
21. Schaefer, E. J., S. Lamon-Fava, J. M. Ordovas, S. D. Cohn, M. M. Schaefer, W. P. Castelli, and P. W. F. Wilson. 1994. Factors associated with low and elevated plasma high density lipo-protein cholesterol and apolipoprotein A-I levels in the Framingham Offspring Study. *J. Lipid Res.* **35:** 871–882.
22. Brousseau, M. E., E. J. Schaefer, J. Dupuis, B. Eustace, P. Van Eerdewegh, A. L. Goldkamp, L. M. Thurston, M. G. FitzGerald, D. Yasek-McKenna, G. O'Neill, G. P. Eberhart, B. Weiffenbach, J. M. Ordovas, M. W. Freeman, R. H. Brown, Jr., and J. Z. Gu. 2000. Novel mutations in the gene encoding ATP-binding cassette 1 in four Tangier disease kindreds. *J. Lipid Res.* **41:** 433–441.
23. Schaefer, E. J. 1984. Clinical, biochemical, and genetic features in familial disorders of high density lipoprotein deficiency. *Arteriosclerosis.* **4:** 303–322.
24. Contois, J. H., J. R. McNamara, C. J. Lammi-Keefe, P. W. F. Wilson, T. Massov, and E. J. Schaefer. 1996. Reference intervals for plasma apolipoprotein A-I determined with a standardized commercial immunoturbidimetric assay: results from the Framingham Offspring Study. *Clin. Chem.* **42:** 507–514.
25. Lathrop, G. M., J. M. Lalauel, C. Julier, and J. Ott. 1985. Multilocus linkage analysis in humans: detection of linkage and estimation of recombination. *Am. J. Hum. Genet.* **37:** 482–498.
26. Boehnke, M. 1991. Allele frequency estimation from data on relatives. *Am. J. Hum. Genet.* **48:** 22–25.
27. Sobel, E., and K. Lange. 1996. Descent graphs in pedigree analysis: applications to haplotyping, location scores, and marker-sharing statistics. *Am. J. Hum. Genet.* **58:** 1323–1337.
28. McNamara, J. R., and E. J. Schaefer. 1987. Automated enzymatic standardized lipid analyses for plasma and lipoprotein fractions. *Clin. Chim. Acta.* **166:** 1–8.
29. Warnick, G. R., J. Benderson, and J. J. Albers. 1982. Dextran sulfate-Mg^{2+} precipitation procedure for quantitation of high-density lipoprotein cholesterol. *Clin. Chem.* **28:** 1379–1388.
30. Otvos, J. D., E. J. Jeyarajah, D. W. Bennett, and R. M. Krauss. 1992. Development of a proton nuclear magnetic resonance spectroscopic method for determining plasma lipoprotein concentrations and subspecies distributions from a single, rapid measurement. *Clin. Chem.* **38:** 1632–1638.
31. Otvos, J. D. 1997. Measurement of lipoprotein subclass profile by nuclear magnetic resonance. *In* Handbook of Lipoprotein Testing. N. Rifai, G. R. Warnick, and M. H. Dominiczak, editors. AACC Press, Washington, D.C. 497–508.
32. Asztalos, B. F., C. H. Sloop, L. Wong, and P. S. Roheim. 1993. Two-dimensional electrophoresis of plasma lipoproteins: recognition of new apoA-I-containing subpopulations. *Biochim. Biophys. Acta.* **1169:** 291–300.
33. Asztalos, B. F., and P. S. Roheim. 1995. Presence and formation of free apolipoprotein A-I-like particles in human plasma. *Arterioscler. Thromb. Vasc. Biol.* **15:** 1419–1423.
34. Asztalos, B. F., C. H. Sloop, L. Wong, and P. S. Roheim. 1993. Comparison of apoA-I-containing subpopulations of dog plasma and prenodal peripheral lymph: evidence for alteration in subpopulations in the interstitial space. *Biochim. Biophys. Acta.* **1169:** 301–304.
35. Havel, R., H. Eder, and J. Bragdon. 1955. The distribution and chemical composition of ultracentrifugally separated lipoproteins in human serum. *J. Clin. Invest.* **34:** 1345–1353.
36. Mendez, A. J., G. M. Anantharamaiah, J. P. Segrest, and J. F. Oram. 1994. Synthetic amphipathic helical peptides that mimic apolipoprotein A-I in clearing cellular cholesterol. *J. Clin. Invest.* **94:** 1698–1705.
37. Lowry, O. H., N. J. Rosebrough, A. L. Farr, and R. J. Randall. 1951. Protein measurement with the Folin phenol reagent. *J. Biol. Chem.* **193:** 265–275.
38. Mendez, A. J., and L. Uint. 1996. Apolipoprotein-mediated cellular cholesterol and phospholipid efflux depend on a functional Golgi apparatus. *J. Lipid Res.* **37:** 2510–2524.
39. Eberhart, G. P., A. J. Mendez, and M. W. Freeman. 1998. Decreased cholesterol efflux from fibroblasts of a patient without Tangier disease, but with markedly reduced high density lipoprotein cholesterol levels. *J. Clin. Endocrinol. Metab.* **83:** 836–846.
40. Francis, G. A., R. H. Knopp, and J. F. Oram. 1995. Defective removal of cellular cholesterol and phospholipids by apolipoprotein A-I in Tangier disease. *J. Clin. Invest.* **96:** 78–87.
41. Assmann, G., O. Simantke, H-E. Schaefer, and E. Smootz. 1977. Characterization of high density lipoproteins in patients heterozygous for Tangier disease. *J. Clin. Invest.* **60:** 1025–1035.
42. Asztalos, B. F., M. Lefevre, T. A. Foster, R. Tulley, M. Windhauser, L. Wong, and P. S. Roheim. 1997. Normolipidemic subjects with low HDL cholesterol levels have altered HDL subpopulations. *Arterioscler. Thromb. Vasc. Biol.* **17:** 1885–1893.
43. Puchois, P., A. Kandoussi, P. Fievet, J. L. Fourrier, M. Bertrand, E. Koren, and J. C. Fruchart. 1987. Apolipoprotein A-I-containing lipoproteins in coronary artery disease. *Atherosclerosis.* **68:** 35–40.
44. Young, S. G., and C. J. Fielding. 1999. The ABC's of cholesterol efflux. *Nature Genet.* **22:** 316–318.
45. Horowitz, B. S., I. J. Goldberg, J. Merab, T. M. Vanni, R. Ramakrishnan, and H. N. Ginsberg. 1993. Increased plasma and renal clearance of an exchangeable pool of apolipoprotein A-I in subjects with low levels of high density lipoprotein cholesterol. *J. Clin. Invest.* **91:** 1743–1752.
46. Brinton, E. A., S. Eisenberg, and J. L. Breslow. 1989. Elevated high density lipoprotein cholesterol levels correlate with decreased apolipoprotein A-I and A-II fractional catabolic rate in women. *J. Clin. Invest.* **84:** 262–269.
47. Brinton, E. A., S. Eisenberg, and J. L. Breslow. 1994. Human HDL cholesterol levels are determined by apoA-I fractional catabolic rate, which correlates inversely with HDL particle size. *Arterioscler. Thromb.* **14:** 707–720.
48. Brousseau, M. E., S. Santamarina-Fojo, L. A. Zech, A. M. Berard,

B. L. Vaisman, S. M. Meyn, D. Powell, H. B. Brewer, and J. M. Hoeg. 1996. Hyperalphalipoproteinemia in human lecithin cholesterol acyltransferase transgenic rabbits. *J. Clin. Invest.* **97:** 1844–1851.
49. Rader, D. J., G. Castro, L. A. Zech, J. C. Fruchhart, and H. B. Brewer. 1991. In vivo metabolism of apolipoprotein A-I on high density lipoprotein particles LpA-I and LpA-I.AII. *J. Lipid Res.* **32:** 1849–1859
50. Schaefer, E. J., L. A. Zech, L. L. Jenkins, T. J. Bronzert, E. A. Rubalcaba, R. T. Lindgren, R. L. Aamodt, and H. B. Brewer. 1982. Human apolipoprotein A-I and A-II metabolism. *J. Lipid Res.* **23:** 850–862.
51. Weng, J., N. L. Mata, S. M. Azarian, R. T. Tzekov, D. G. Birch, and G. H. Travis. 1999. Insights into the function of Rim protein in photoreceptors and etiology of Stargardt's disease from the phenotype in abcr knockout mice. *Cell.* **98:** 13–23.
52. Francis, G. A., R. H. Knopp, and J. F. Oram. 1995. Defective removal of cellular cholesterol and phospholipids by apolipoprotein A-I in Tangier disease. *J. Clin. Invest.* **96:** 78–87.
53. Remaley, A. T., S. Rust, M. Rosier, C. Knapper, L. Naudin, C. Broccardo, K. M. Peterson, C. Koch, I. Arnould, C. Prades, N. Duverger, H. Funke, G. Assmann, M. Dinger, M. Dean, G. Chimini, S. Santamarina-Fojo, D. S. Fredrickson, P. Denefle, and H. B. Brewer, Jr. 1999. Human ATP-binding cassette transporter 1 (ABC1): genomic organization and identification of the genetic defect in the original Tangier disease kindred. *Proc. Natl. Acad. Sci. USA.* **96:** 12685–12690.
54. Almasy, L., J. E. Hixson, D. L. Rainwater, S. Cole, J. T. Williams, M. C. Mahaney, J. L. VandeBerg, M. P. Stern, M. W. MacCluer, and J. Blangero. 1999. Human pedigree-based quantitative-trait-locus mapping: localization of two genes influencing HDL-cholesterol metabolism. *Am. J. Hum. Genet.* **64:** 1686–1693.